Structural influence on photochromic behaviors of Eu^{2+}-doped glaserite-type silicates

Yoshinori Yonezaki

Center for Crystal Science and Technology, Graduate Faculty of Interdisciplinary Research, University of Yamanashi, Miyamae 7–32, Kofu 400-8511, Japan

A B S T R A C T

$Ba_{2.98-x}Sr_xEu_{0.02}MgSi_2O_8$ ($x \leq 0.365$) exhibited emission-color change when exposed to the light from a Xe arc-lamp. Blue emission observed from the above phosphors turned purple after the photostimulation because of 608-nm emission centers arising. The degree of the spectral change monotonically decreased with increasing Sr-replacement x, and became undetectable when x exceeded 0.490. This x value coincided with that dividing the structural symmetry between $P\bar{3}$ ($Z = 3$) and $P\bar{3}m1$ ($Z = 1$). This coincidence indicates that structural distortion caused by B-site Ba^{2+} ions contributes to the photostimulated emission-color change of the Eu^{2+}-doped glaserite-type alkali-earth magnesium silicates.

1. Introduction

Since the discovery of radiation dosimetry using K_2SO_4 [1–3], bracelet–type $XY[TO_4]$ compounds (X, Y: 10– and 12–coordinated cations; T: tetrahedrally coordinated cation) have been focused on as optical materials. In particular, glaserite-type $M_3MgSi_2O_8$ (M: Ba, Sr, Ca), which forms a solid solution series over a wide range of Ba: Sr: Ca ratio, have attracted much attention because they show intense blue emissions under ultraviolet (UV) light when Eu^{2+} ions are doped. Their emission properties are understood from the viewpoint of the co-ordination environment around the dopants [4–17]. In such research backgrounds, our group found that $Ba_3MgSi_2O_8$: Eu^{2+} exhibited photochromic behaviors [18,19]. After UV-light photostimulation, as-made colorless $Ba_3MgSi_2O_8$: Eu^{2+} turned orange, and simultaneously, the emission color changed from blue to purple. The following heat treatment or blue-to-green laser irradiation restored original absorption and emission characters. Such easily-achievable reversible changes enable repeatable switching of the optical properties by external stimulation. According to our previous studies, the emission-color change originates in photoinduced red-emitting centers. When $Ba_3MgSi_2O_8$: Eu^{2+} is exposed to UV light, electrons in valence states are once excited, and then, decay near Eu^{2+} ions. Since the transition energies among the eigenstates of the Eu^{2+}-associated electron (F_A center) correspond to visible range, the photostimulated material shows the different color and emission from the original. It should be noted that the photostimulation wavelengths which could facilitate the emission-color change fell within the Urbach edge of $Ba_3MgSi_2O_8$. This fact indicates that a sequence of the coloring reactions might have been initiated by a photoexcitation involving localized states of some structural disorders [19].

However, such structure-property relationship has not been verified yet. In this study, we investigated the photochromic characters of Eu^{2+}-doped (Ba, Sr)$_3MgSi_2O_8$ solid solution and identified Ba^{2+}: Sr^{2+} range on which the emission-color changed by photostimulation. By comparing the range with other spectroscopic data, structural features necessary for inducing the red-emitting centers are discussed.

2. Experimental

2.1. Synthesis

The polycrystalline powder samples of $Ba_{2.98-x}Sr_xEu_{0.02}MgSi_2O_8$ ($x = 0–0.990$) were prepared from reagent grade barium carbonate, magnesium carbonate hydroxide, silica and europium (III) oxide. A small amount of ammonium chloride was used as a flux. Stoichiometric amounts of the reagents and the flux were ground and mixed by ball milling with zirconia beads in 2-propanol for 4 h. The mixture was heated at 1100 °C for 4 h in a flow of $4\%H_2-96\%N_2$ gas with an intermittent re-grinding to obtain expected products.

2.2. Phase identification

The samples ground with mortar and pestle were investigated by x–ray powder diffraction at room temperature using $CuK\alpha$ radiation ($\lambda = 1.5418$ Å) with a Rigaku Multiflex diffractometer to check the crystalline phases involved in the samples.
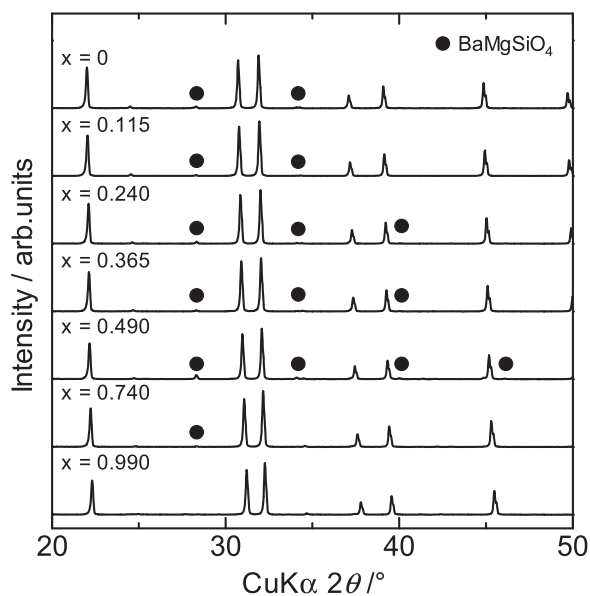
Fig. 1. X–ray powder diffraction patterns of $Ba_{2.98-x}Sr_xEu_{0.02}MgSi_2O_8$ ($x = 0$–0.990). The reflection peaks of an impurity phase are marked with closed circles. An extended figure ($30° \leq 2\theta \leq 40°$ range) is attached as a Supplementary material to show systematic peak-shift clearly.

2.3. Electron spin resonance (ESR) spectroscopy

ESR spectroscopy was performed for the samples on a JES-RE3X X-band ESR spectrometer (JEOL Co., Ltd) which utilized 100 kHz magnetic field modulation. MgO: Mn^{2+} was used as a standard for g-factor correction. A powder sample was put into a silica tube, and ESR measurement was performed on it at room temperature. Spin density of each sample was determined by comparing signal intensities of the sample and a coal with known spin density.

2.4. Raman spectroscopy

Raman spectra were measured for the samples at room temperature in backscattering geometry by a 3000 grooves mm^{-1} grating monochromator and charge-coupled device detector system (RENISHAW, inVia Reflex system). Samples were excited with the 488-nm line of a 50 mW Spectra–Physics Cyan™ Scientific CW laser. The laser beam was focused on a sample surface by a $50\times$ objective lens. A spectral resolution was 0.5 cm^{-1}. The laser power was attenuated to 5 mW before the irradiation. The obtained data were used for checking the site symmetries on which SiO_4 motifs located.

2.5. Photostimulation procedure

In order to facilitate photochemical reactions, powder samples were irradiated with a 150 W Xe arc-lamp set in lamp house (Hamamatsu photonics L2273, E2420) for a desired period. The Xe-lamp window was set 2 cm above a sample surface.

2.6. Emission spectroscopy

Emission and excitation spectra were measured for the prepared samples at room temperature using a spectrofluorometer with a Xe-lamp as an excitation source (FP–6500, JASCO).
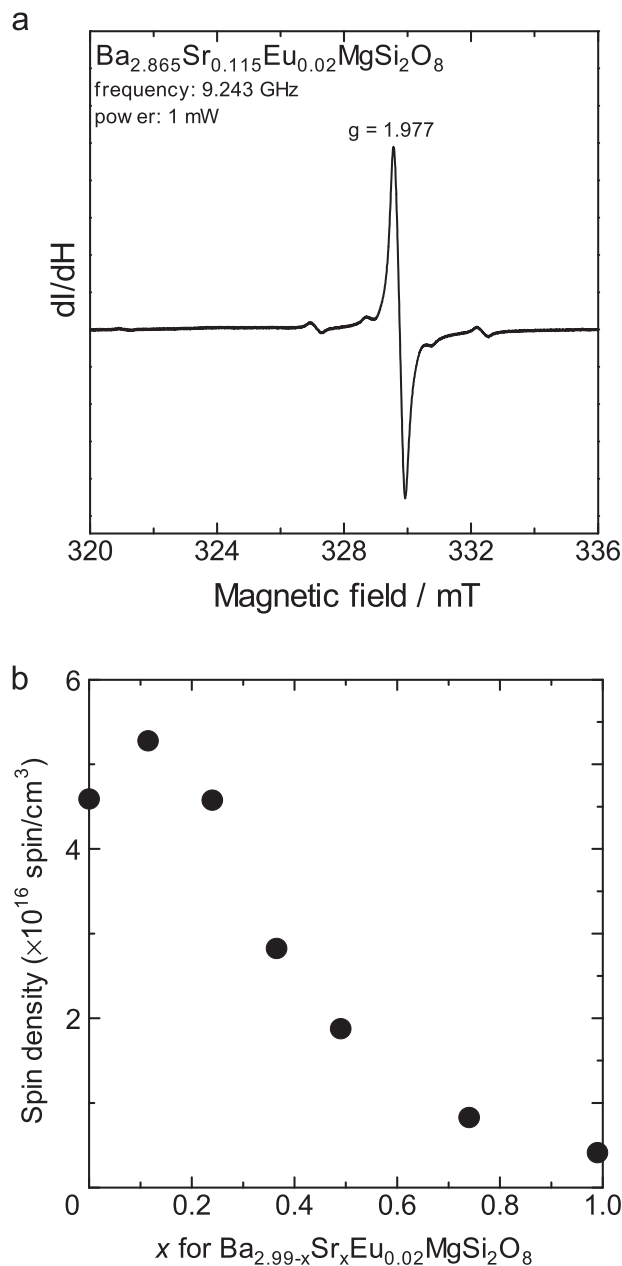

Fig. 2. (a) ESR spectrum of the sample of $x = 0.115$. (b) Sr-replacement dependence of spin density of the unpaired electrons within $BaMgSiO_4$ impurity phase.

3. Results

3.1. Structural aspects on Eu^{2+}-doped $(Ba, Sr)_3MgSi_2O_8$ solid solution

Fig. 1 shows the XRD patterns of $Ba_{2.98-x}Sr_xEu_{0.02}MgSi_2O_8$ samples. The obtained patterns agreed with previous data for $(Ba, Sr)_3MgSi_2O_8$ solid solution series [20]. The diffraction peaks systematically shifted to higher 2θ angle with increasing Sr–ratio, which indicates that small Sr^{2+} ions successfully replaced large Ba^{2+} ions. A trace of $BaMgSiO_4$ was observed for the samples of $x \leq 0.740$. This impurity formation was due to a minor compositional deviation from the stoichiometry of the main phase [12,20]. For Ba-rich side of $Ba_{2.98-x}Sr_xEu_{0.02}MgSi_2O_8$, a small proportion of Ba^{2+} ions were excluded from relatively small alkali-earth sites because of the size mismatch. As a result, the excluded ions formed $BaMgSiO_4$, and vacancies were left within the main phase. Therefore, $BaMgSiO_4$ should be a measure of the vacancy involved in $Ba_{2.98-x}Sr_xEu_{0.02}MgSi_2O_8$. Fig. 2a shows the ESR spectrum of